

**Supporting Information**  
for  
**“A Combined First Principles and Experimental Approach to  
Bi<sub>2</sub>WO<sub>6</sub>”**

Quazi Shafayat Hossain,<sup>1</sup> Sadiq Shahriyar Nishat,<sup>2</sup> Mohsina Sultana,<sup>1</sup> Tasnim  
Ahmed Mahi,<sup>1,3</sup> Shahrar Ahmed,<sup>1,4</sup> M. N. I. Khan,<sup>5</sup> H. N. Das,<sup>5</sup> Muhammad  
Shahriar Bashar,<sup>6</sup> Umme Sarmeen Akhtar,<sup>7</sup> Sharmin Jahan,<sup>8</sup> Fariha Chowdhury,<sup>9</sup>  
Khandker Saadat Hossain,<sup>10</sup> Sazzad M.S. Imran,<sup>1</sup> and Imtiaz Ahmed<sup>1,\*</sup>

<sup>1</sup>*Materials Science Research Laboratory,  
Department of Electrical and Electronic Engineering,  
University of Dhaka, Dhaka-1000, Bangladesh*

<sup>2</sup>*Department of Materials Science and Engineering,  
Rensselaer Polytechnic Institute, Troy, NY, USA*

<sup>3</sup>*Semiconductor Technology Research Centre,  
University of Dhaka, Dhaka-1000, Bangladesh*

<sup>4</sup>*Institute of Mining, Mineralogy and Metallurgy,  
Bangladesh Council of Scientific and Industrial Research, Joypurhat-5900, Bangladesh*

<sup>5</sup>*Materials Science Division, Atomic Energy Centre, Dhaka-1000, Bangladesh*

<sup>6</sup>*Institute of Energy Research and Development,  
Bangladesh Council of Scientific and Industrial Research, Dhaka-1205, Bangladesh*

<sup>7</sup>*Institute of Glass and Ceramic Research and Testing,  
Bangladesh Council of Scientific and Industrial Research, Dhaka-1205, Bangladesh*

<sup>8</sup>*Institute of Energy Science and Technology,  
Bangladesh Council of Scientific and Industrial Research, Dhaka-1205, Bangladesh*

<sup>9</sup>*Biomedical and Toxicological Research Institute,  
Bangladesh Council of Scientific and Industrial Research, Dhaka-1205, Bangladesh*

<sup>10</sup>*Nanophysics and Soft Matter Laboratory, Department of Physics,  
University of Dhaka, Dhaka-1000, Bangladesh*

## I. XRD ANALYSIS

---

\* imtiaz@du.ac.bd

Crystallographic Parameters, Bond Lengths and Bond Angles												
Sample/DFT	Sym.	$a$ (Å)	$b$ (Å)	$c$ (Å)	$\alpha$ (°)	$\beta$ (°)	$\gamma$ (°)	$V$ (Å <sup>3</sup> )	$d_{W-O}$ (Å)	$d_{Bi-O}$ (Å)	$\chi^2$	
SBWO	$Pca2_1$	5.433	16.415	5.454	90	90	90	486.442	1.797, 1.803, 1.859	2.182, 2.242, 2.302	1.75	
									1.862, 2.135, 2.144	2.441, 2.498, 2.500		
HBWO-U	$Pca2_1$	5.449	16.348	5.450	90	90	90	485.487	1.806, 1.853	2.180, 2.241, 2.300	1.45	
									2.135, 2.147	2.438, 2.500, 2.502		
HBWO-S	$Pca2_1$	5.452	16.340	5.440	90	90	90	484.601	1.805, 1.852	2.179, 2.240, 2.298	1.27	
									1.854, 2.133, 2.146	2.434, 2.498, 2.502		
GGA-PBE	$Pca2_1$	5.551	16.882	5.591	90	90	90	523.938	1.819, 1.886	1.791, 1.815, 1.851		
									1.889, 2.204, 2.216	1.887, 2.142, 2.209		
GGA-PBE+ $U_d$ (2 eV)+ $U_p$ (2 eV)	$Pca2_1$	5.515	16.979	5.558	90	90	90	520.393	1.895, 1.901, 1.902	1.831, 1.846, 1.893		
									1.903, 2.021, 2.027	1.922, 1.9898, 2.160		
GGA-PBE+ $U_d$ (5 eV)+ $U_p$ (5 eV)	$Pca2_1$	5.468	17.111	5.514	90	90	90	515.931	1.895, 1.901, 1.902	1.864, 1.887, 1.900		
									1.903, 2.021, 2.027	1.926, 1.987, 2.085		
GGA-PBE+ $U_d$ (7 eV)+ $U_p$ (7 eV)	$Pca2_1$	5.438	17.206	5.488	90	90	90	513.416	1.895, 1.901, 1.902	1.897, 1.899, 1.904		
									1.903, 2.021, 2.027	1.925, 1.967, 2.028		
GGA-PBE+ $U_d$ (9 eV)+ $U_p$ (9 eV)	$Pca2_1$	5.422	17.263	5.477	90	90	90	512.634	1.895, 1.901, 1.902	1.907, 1.918, 1.924		
									1.903, 2.021, 2.027	1.937, 1.954, 1.991		
GGA-PBE+ $U_d$ (12 eV)+ $U_p$ (12 eV)	$Pca2_1$	5.408	17.340	5.478	90	90	90	513.716	1.895, 1.901, 1.902	1.910, 1.923, 1.941		
									1.903, 2.021, 2.027	1.952, 1.964, 1.974		
GGA-PBE+ $U_d$ (14 eV)+ $U_p$ (14 eV)	$Pca2_1$	5.401	17.404	5.482	90	90	90	515.284	1.895, 1.901, 1.902	1.912, 1.922, 1.946		
									1.903, 2.021, 2.027	1.954, 1.961, 1.970		

TABLE S1. Crystallographic parameters of SBWO, HBWO-U, and HBEO-S samples along with that of GGA-PBE and GGA-PBE+ $U_d$ + $U_p$  for different values of  $U_d$  and  $U_p$ .

Crystallographic Parameters, Bond Lengths and Bond Angles											
Sample/DFT	Sym.	$a(\text{Å})$	$b(\text{Å})$	$c(\text{Å})$	$\alpha(^{\circ})$	$\beta(^{\circ})$	$\gamma(^{\circ})$	$V(\text{Å}^3)$	$d_{\text{W-O}}(\text{Å})$	$d_{\text{Bi-O}}(\text{Å})$	$\chi^2$
SBWO	$Pca2_1$	5.43316	4.15545	4.54900	90	90	90	486.442	1.797, 1.803, 1.8592	1.182, 2.242, 2.302	1.75
									1.862, 2.135, 2.1442	2.441, 2.498, 2.500	
HBWO-U	$Pca2_1$	5.44916	3.34854	4.50900	90	90	90	485.487	1.799, 1.806, 1.8532	1.180, 2.241, 2.300	1.45
									1.855, 2.135, 2.1472	2.438, 2.500, 2.502	
HBWO-S	$Pca2_1$	5.45216	3.34054	4.40900	90	90	90	484.601	1.797, 1.805, 1.8522	1.179, 2.240, 2.298	1.27
									1.854, 2.133, 2.1462	2.434, 2.498, 2.502	
GGA-PBE+vdW	$Pca2_1$	5.50816	6.16551	7.90000	90	90	90	504.921	1.819, 1.819, 1.8832	2.214, 2.275, 2.340	
									1.883, 2.158, 2.1582	2.469, 2.499, 2.517	
GGA-PBE+ $U_d$ (2 eV)+ $U_p$ (2 eV)+vdW	$Pca2_1$	5.48316	6.66754	8.88900	90	90	90	501.493	1.835, 1.835, 1.8882	2.209, 2.275, 2.328	
									1.888, 2.114, 2.1142	2.485, 2.492, 2.506	
GGA-PBE+ $U_d$ (5 eV)+ $U_p$ (5 eV)+vdW	$Pca2_1$	5.44016	8.00545	1.90000	90	90	90	498.105	1.869, 1.869, 1.8952	2.203, 2.277, 2.304	
									1.895, 2.044, 2.0442	2.475, 2.494, 2.508	
GGA-PBE+ $U_d$ (7 eV)+ $U_p$ (7 eV)+vdW	$Pca2_1$	5.41616	8.68543	2.90000	90	90	90	496.216	1.898, 1.898, 1.9002	1.199, 2.283, 2.287	
									1.900, 1.996, 1.9962	2.457, 2.484, 2.536	
GGA-PBE+ $U_d$ (9 eV)+ $U_p$ (9 eV)+vdW	$Pca2_1$	5.40416	9.13542	3.90000	90	90	90	495.778	1.900, 1.900, 1.9192	1.192, 2.274, 2.287	
									1.919, 1.971, 1.9712	2.444, 2.486, 2.551	
GGA-PBE+ $U_d$ (12 eV)+ $U_p$ (12 eV)+vdW	$Pca2_1$	5.39316	9.63542	4.90000	90	90	90	496.259	1.902, 1.902, 1.9322	1.180, 2.261, 2.285	
									1.932, 1.958, 1.9582	2.431, 2.503, 2.548	
GGA-PBE+ $U_d$ (14 eV)+ $U_p$ (14 eV)+vdW	$Pca2_1$	5.38717	10.07542	5.90000	90	90	90	497.051	1.895, 1.895, 1.9042	1.169, 2.254, 2.282	
									1.935, 1.956, 1.9562	2.424, 2.523, 2.535	

TABLE S2. Crystallographic parameters of SBWO, HBWO-U, and HBEO-S samples along with that of GGA-PBE+vdW and GGA-PBE+ $U_d$ + $U_p$ +vdW for different values of  $U_d$  and  $U_p$ . The van der Waals (vdW) interaction was included with the DFT-D3 method including Becke-Johnson (B-J) damping.

## II. RAMAN ANALYSIS

TABLE S3. RT experimental Raman peaks of SBWO, HBWO-U, and HBWO-S samples along with that of DFT (GGA-PBE and GGA-PBE+ $U_d+U_p$ ) simulations. ELM: External Lattice Mode, AD: Asymmetric Distortion, SBV: Symmetric Bending Vibrations, ABV: Asymmetric Bending Vibrations, TM: Translational Mode, ABrM: Asymmetric Bridging Mode, AST: Asymmetric Stretching.

Raman Peak Analysis						
SBWO	HBWO-U	HBWO-S	GGA-PBE	GGA-PBE+ $U_d+U_p$	Symm.	Peak Assignment
( $\text{cm}^{-1}$ )	( $\text{cm}^{-1}$ )	( $\text{cm}^{-1}$ )	( $\text{cm}^{-1}$ )	( $\text{cm}^{-1}$ )		
-	129	139	129	128	$E_g$	ELM
153	152	152	154	158	$A_{1g}$	ELM
-	222	225	222	228	$B_{1g}$	WO <sub>6</sub> AD
242	255	260	254	260	$A_{1g}$	Bi-O SBV
283	282	283	274	282	$E_g$	WO <sub>6</sub> ABV
295	300	306	296	298	$E_g$	Bi <sup>3+</sup> and WO <sub>6</sub> <sup>6-</sup> TM
406	413	417	408	412	$E_g$	WO <sub>6</sub> ABV
711	716	704	713	716	$B_{1g}$	WO <sub>6</sub> ABrM
-	-	724	731	732	$B_{1g}$	O-W-O AST
800	796	796	794	804	$B_{1g}$	WO <sub>6</sub> ABrM
-	814	821	811	834	$B_{1g}$	O-W-O AST

## III. FTIR ANALYSIS

TABLE S4. The SBWO, HBWO-U, and HBWO-S samples' FTIR peak designations to corresponding atomic motion along with DFT-derived peaks of phonon density of states for GGA-PBE+vdW and GGA-PBE+ $U_d+U_p$ +vdW. SV: Symmetric Vibration, AST: Asymmetric Stretching, SST: Symmetric Stretching, BV: Bending Vibration.

FTIR Peak Analysis						
SBWO	HBWO-U	HBWO-S	GGA-PBE+vdW	GGA-PBE+ $U_d+U_p$ +vdW		Peak Assignment
( $\text{cm}^{-1}$ )	( $\text{cm}^{-1}$ )	( $\text{cm}^{-1}$ )	( $\text{cm}^{-1}$ )	( $\text{cm}^{-1}$ )		
417	427	427	419	424		Bi-O SST
533	565	565	526	540		Bi-O-Bi AST
680	703	697	684	678		W-O SST
818	812	820	782	814		Bi-O SST
958	-	-	915	930		O-H BV
1056	1026	1029	-	-		W-O SST
-	1108	-	-	-		C-C SST
-	1314	1392	-	-		C=O SST
-	1636	1627	-	-		O-H SST
-	3471	3469	-	-		O-H BV

#### IV. EDX ANALYSIS

The EDX spectra in Fig. S1 presents the characteristic peaks of X-ray radiation for Bi ( $L_\alpha = 10.79$  keV,  $L_\beta = 13.00$  keV,  $M_\alpha = 2.42$  keV, W ( $L_\alpha = 8.25$  keV,  $L_\beta = 9.75$  keV, and  $M_\alpha = 1.85$  keV) in all samples.

TABLE S5. Chemical species identification, atomic percentage at. (%) and weight percentage wt. (%) concentration analysis using EDX (Model: EDAX Team) of SBWO, HBWO-U, and HBWO-S.

EDX Analysis					
Sample	Element	at. (%) (Theory)	at. (%) (Exp.)	wt. (%) (Theory)	wt. (%) (Exp.)
SBWO	Bi	22.22	22.8	59.89	59
	W	11.11	10.79	26.35	27.31
	O	66.67	66.41	13.76	13.69
HBWO-U	Bi	22.22	22.39	59.89	59.89
	W	11.11	11.12	26.35	26.66
	O	66.67	66.49	13.76	13.45
HBWO-S	Bi	22.22	22.16	59.89	59.9
	W	11.11	11.37	26.35	26.38
	O	66.67	66.47	13.76	13.72

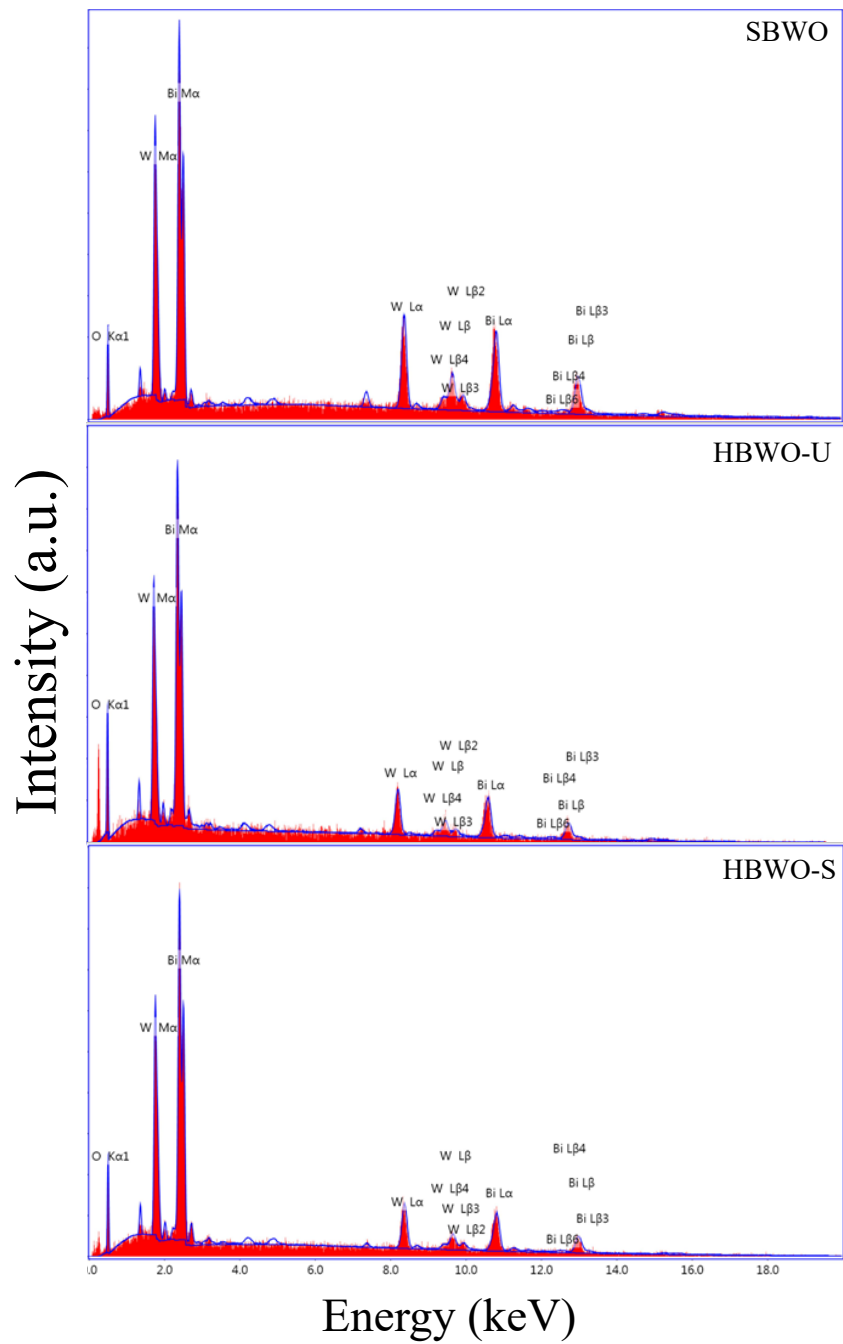


FIG. S1. EDX spectra of (a) SBWO, (b) SBWO-U, and (c) SBWO-S measured by EDX Model: EDAX Team machine.

## V. ELECTRONIC PROPERTIES SIMULATION

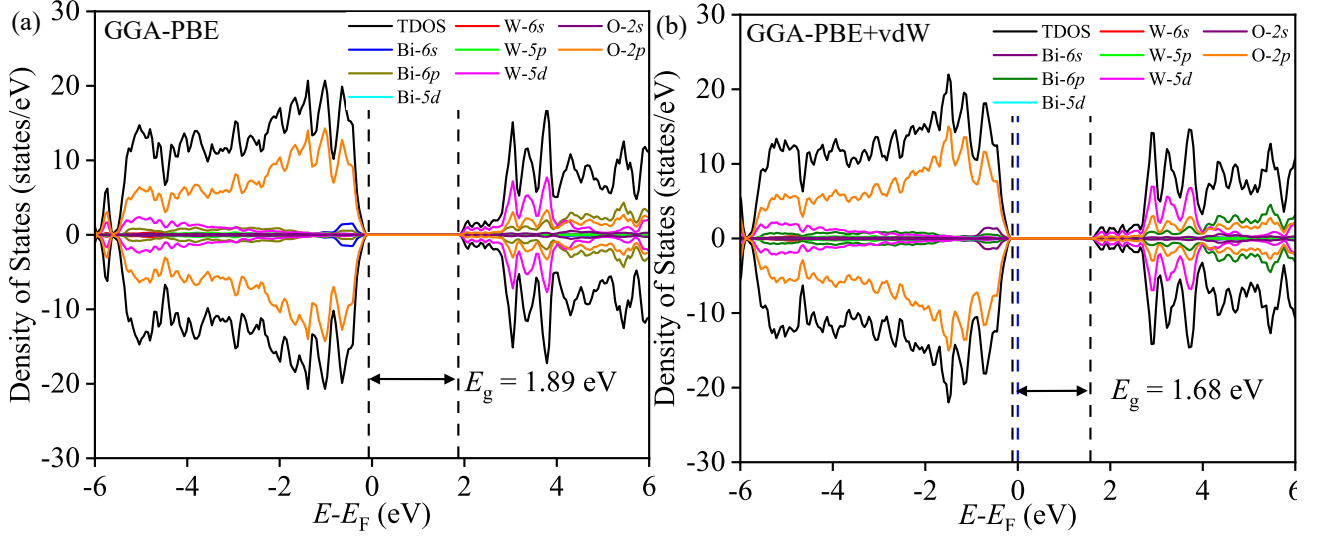


FIG. S2. TDOS and PDOS of BWO for (a) GGA-PBE and (b) GGA-PBE+vdW functionals. The inclusion of vdW force reduces the band gap  $E_g$  in DOS.

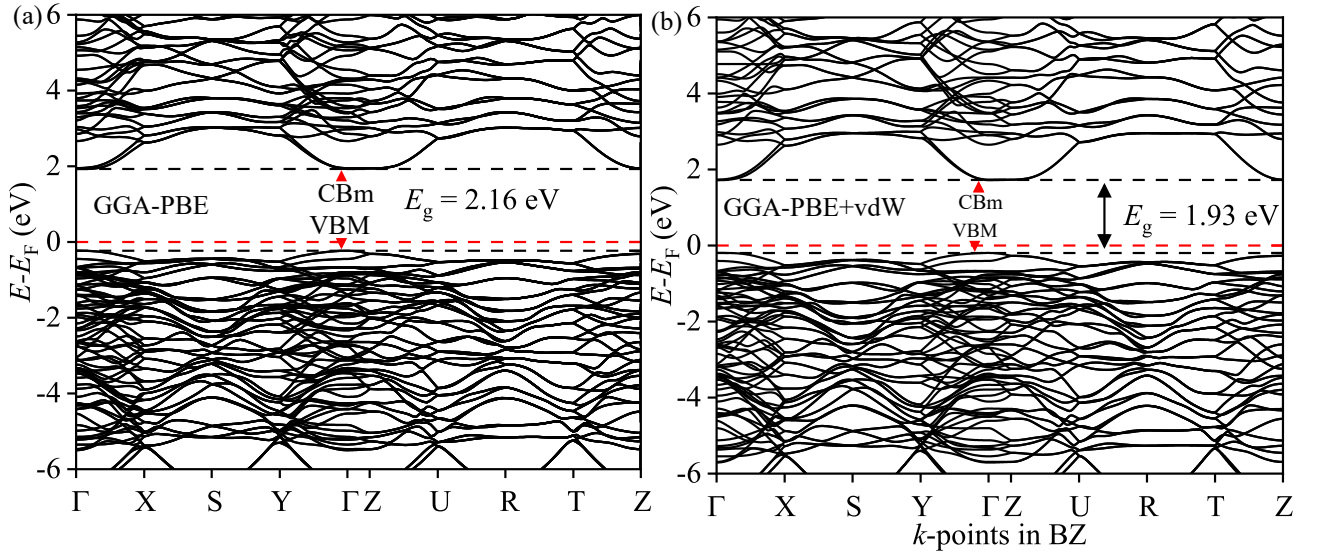


FIG. S3. Electronic BS of BWO for (a) GGA-PBE and (b) GGA-PBE+vdW functionals. The inclusion of vdW force reduces the band gap  $E_g$  in BS. The GGA-PBE predicts the erroneous direct nature of the band gap regardless of the vdW force.

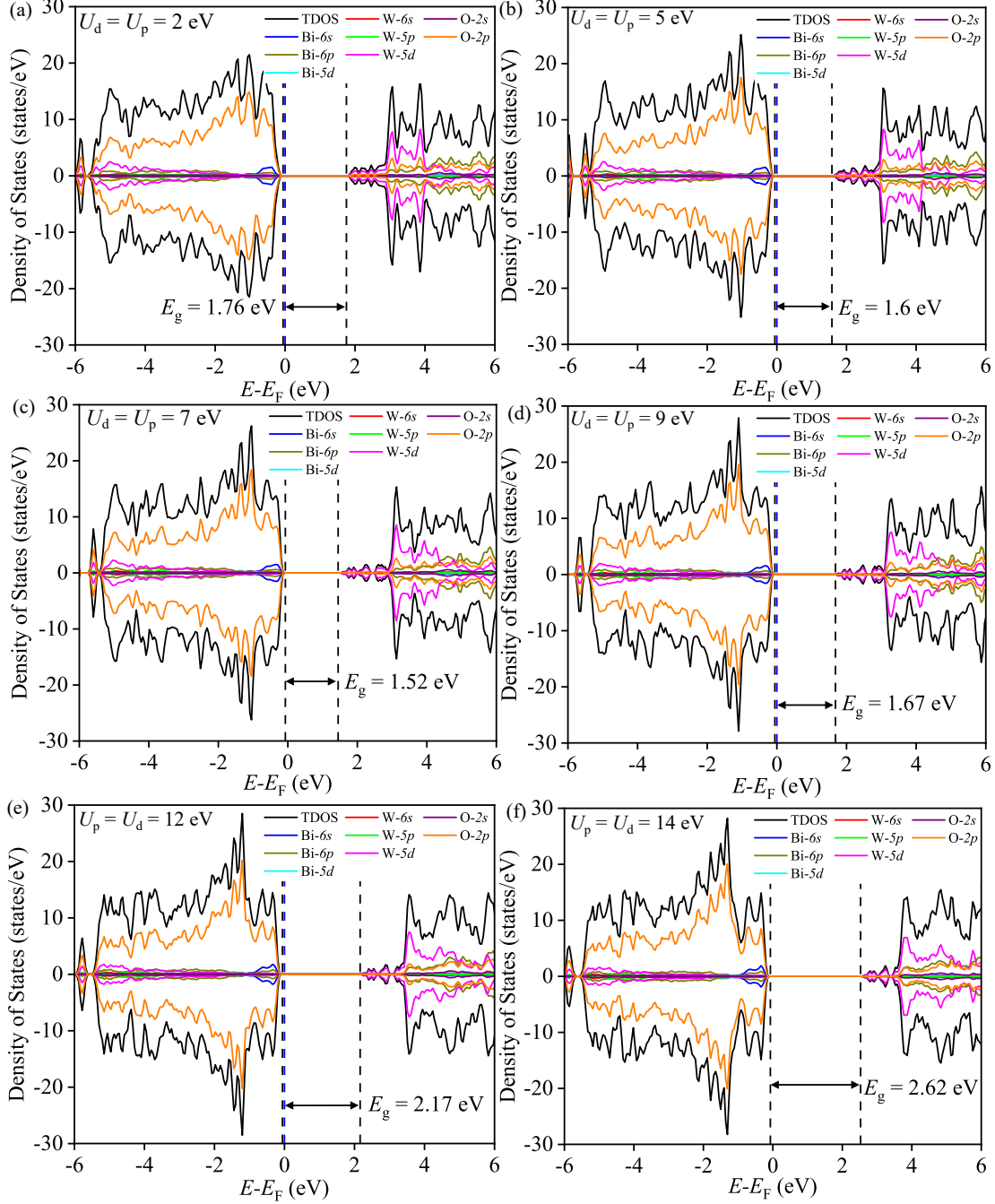


FIG. S4. TDOS and PDOS of BWO for GGA-PBE+ $U_d+U_p$  with (a)  $U_d = U_p = 2$  eV, (b)  $U_d = U_p = 5$  eV, (c)  $U_d = U_p = 7$  eV, (d)  $U_d = U_p = 9$  eV, (e)  $U_d = U_p = 12$  eV and (f)  $U_d = U_p = 14$  eV. The band gap  $E_g$  varies with different values of  $U_d$  and  $U_p$ .



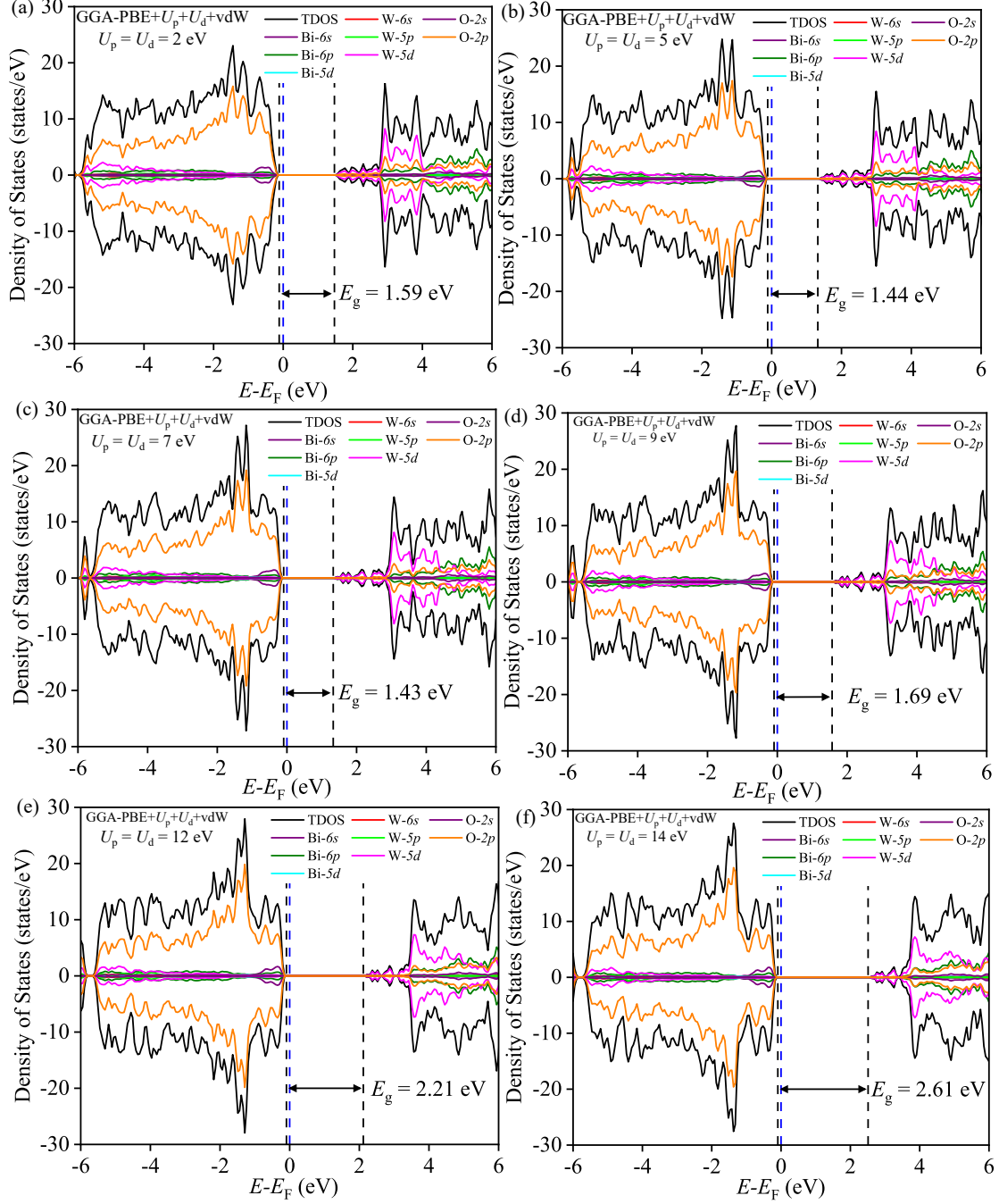


FIG. S5. The vdW force is included. TDOS and PDOS of BWO for GGA-PBE+ $U_d+U_p$ +vdW with (a)  $U_d = U_p = 2$  eV, (b)  $U_d = U_p = 5$  eV, (c)  $U_d = U_p = 7$  eV, (d)  $U_d = U_p = 9$  eV, (e)  $U_d = U_p = 12$  eV and (f)  $U_d = U_p = 14$  eV. The band gap  $E_g$  varies with different values of  $U_d$  and  $U_p$ .

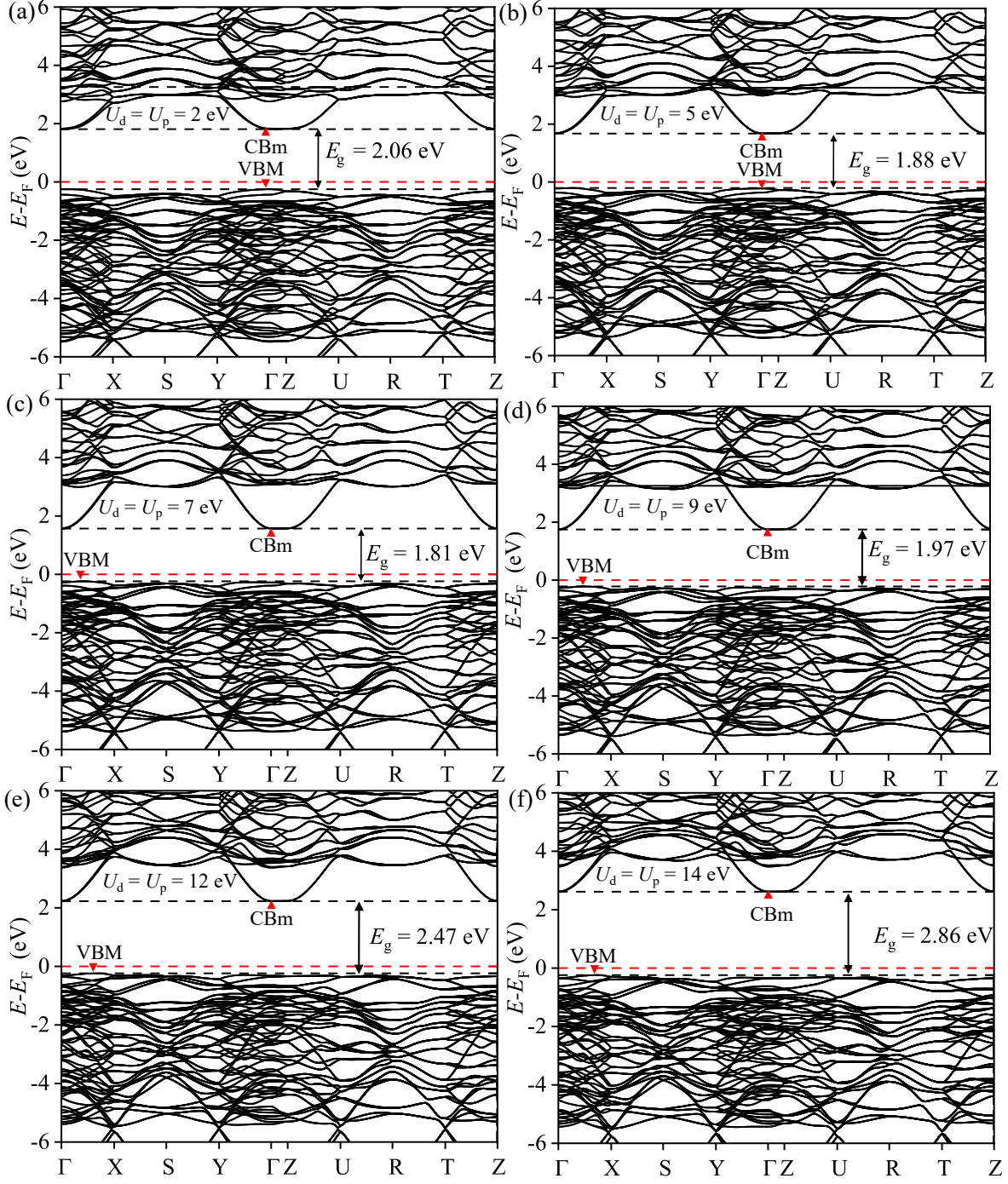


FIG. S6. Electronic BS of BWO in the absence of vdW force for GGA-PBE+ $U_d+U_p$  with (a)  $U_d = U_p = 2$  eV, (b)  $U_d = U_p = 5$  eV, (c)  $U_d = U_p = 7$  eV, (d)  $U_d = U_p = 9$  eV, (e)  $U_d = U_p = 12$  eV and (f)  $U_d = U_p = 14$  eV. The band gap  $E_g$  in the BS varies with different values of  $U_d$  and  $U_p$ .

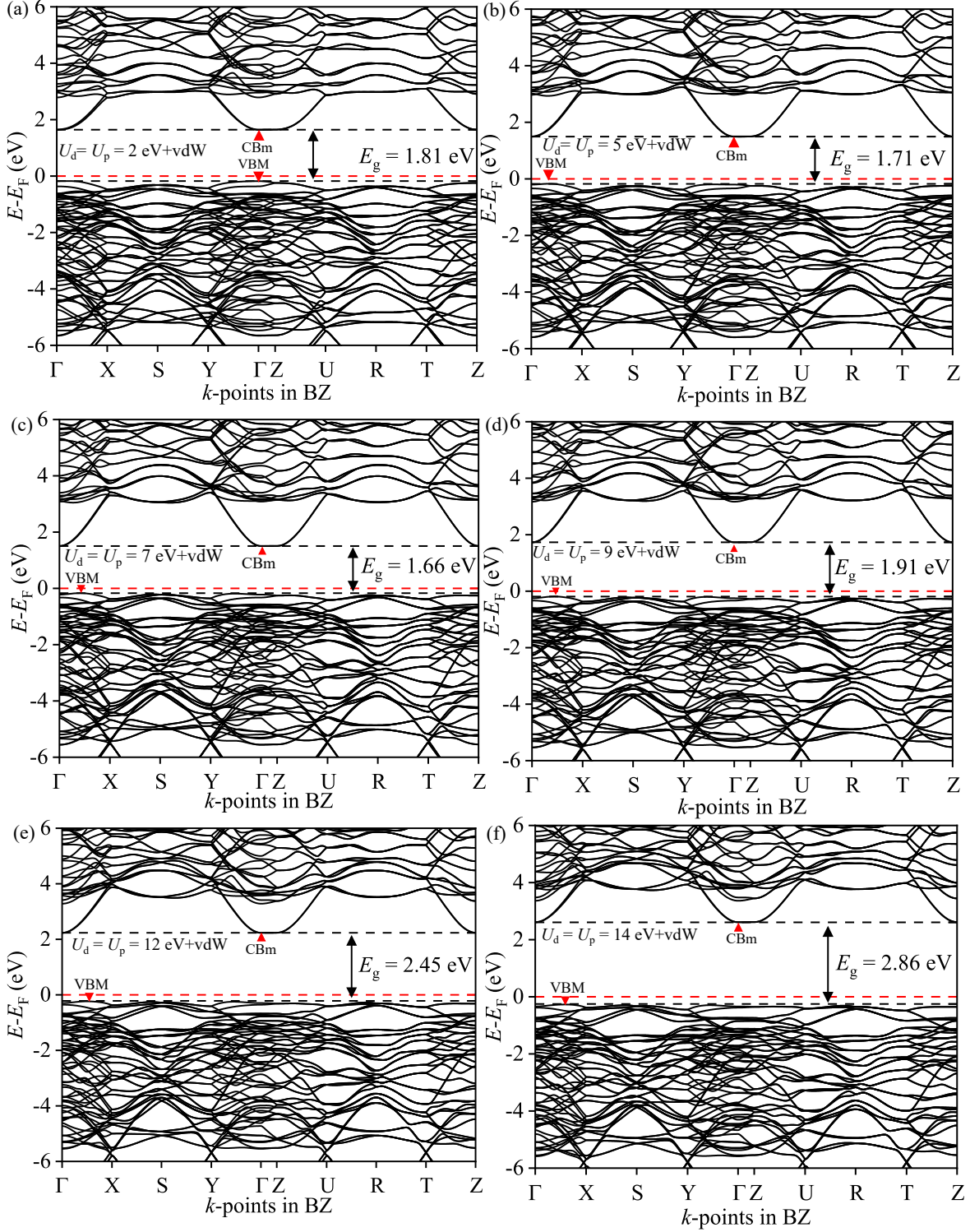


FIG. S7. The vdW force is included. Electronic BS of BWO for GGA-PBE+ $U_d+U_p$ +vdW with (a)  $U_d = U_p = 2$  eV, (b)  $U_d = U_p = 5$  eV, (c)  $U_d = U_p = 7$  eV, (d)  $U_d = U_p = 9$  eV, (e)  $U_d = U_p = 12$  eV and (f)  $U_d = U_p = 14$  eV. The band gap  $E_g$  in the BS varies with different values of  $U_d$  and  $U_p$ .

## VI. ELASTIC PROPERTIES SIMULATION

TABLE S6. Elastic constants ( $C_{ij}$ ), bulk moduli ( $B_V$ ,  $B_R$  and  $B_H$ ), shear moduli ( $G_V$ ,  $G_R$ ,  $G_H$ ), Young's moduli ( $E_V$ ,  $E_R$ ,  $E_H$ ), Poisson's ratio ( $\nu_V$ ,  $\nu_R$ ,  $\nu_H$ ) and Pugh's ratio ( $k_V$ ,  $k_R$ ,  $k_H$ ) in Voigt–Reuss–Hill framework for for BWO using GGA-PBE, GGA-PBE+ $U_d+U_p$  and GGA-PBE+ $U_d+U_p$ +vdW.

Elastic Properties (E.P.) of BWO			
E.P.	GGA-PBE	GGA-PBE+ $U_d+U_p$	GGA-PBE+ $U_d+U_p$ +vdW
$C_{11}$ (GPa)	131.293	201.29	233.269
$C_{12}$ (GPa)	4.028	68.734	90.058
$C_{13}$ (GPa)	42.544	48.644	58.849
$C_{22}$ (GPa)	103.827	190.576	215.771
$C_{23}$ (GPa)	12.643	8.052	18.775
$C_{33}$ (GPa)	98.635	100.703	106.653
$C_{44}$ (GPa)	44.365	36.669	39.994
$C_{55}$ (GPa)	60.567	70.187	80.6
$C_{66}$ (GPa)	33.829	104.078	106.212
$B_V$ (GPa)	50.240	82.600	99.010
$B_R$ (GPa)	48.632	68.254	78.834
$B_H$ (GPa)	49.438	75.428	88.920
$G_V$ (GPa)	46.050	66.660	71.230
$G_R$ (GPa)	43.064	56.286	60.287
$G_H$ (GPa)	44.559	61.474	65.758
$E_V$ (GPa)	105.830	157.590	172.350
$E_R$ (GPa)	99.749	132.449	144.122
$E_H$ (GPa)	102.794	145.024	158.261
$\nu_V$	0.150	0.180	0.210
$\nu_R$	0.158	0.177	0.195
$\nu_H$	0.153	0.180	0.203
$k_V$	1.090	1.240	1.390
$k_R$	1.129	1.213	1.308
$k_H$	1.109	1.227	1.352

## VII. BORN CHARGE

The Born effective charge (BEC) embodies the atomic charge dynamics. The BEC has its origin in the screening of long-range Coulomb potential of the ions whose motion forms the phonon characteristics. The simulated BEC tensor is displayed in Table S7 for both GGA-PBE+vdW and GGA-PBE+ $U_d+U_p$ +vdW.

TABLE S7. Born effective charge tensor of BWO using GGA-PBE+vdW and GGA-PBE+ $U_d+U_p$ +vdW.

	$Z_B$	Position	xx	xy	xz	yx	yy	yz	zx	zy	zz
BWO	Bi	4a	4.779	-0.263	0.495	-0.201	4.793	0.010	0.907	0.536	4.453
GGA-PBE+vdW	Bi	4a	4.781	0.264	0.493	0.202	4.792	-0.011	0.907	-0.536	4.454
	W	4a	8.196	0.005	0.450	-0.003	6.820	0.001	0.411	0.000	7.989
	O1	4a	-2.207	0.042	1.306	0.301	-2.201	0.639	1.214	1.222	-4.509
	O2	4a	-3.699	-2.142	-0.434	-2.112	-3.039	-0.339	-0.404	-0.254	-1.342
	O3	4a	-3.696	2.143	-0.432	2.112	-3.042	0.340	-0.402	0.256	-1.341
	O4	4a	-2.206	0.041	1.305	0.302	-2.202	0.571	1.212	1.225	-4.509
	O5	4a	-2.974	-0.254	0.452	0.117	-2.961	0.150	0.193	0.218	-2.598
	O6	4a	-2.975	0.253	-0.452	-0.116	-2.961	0.150	-0.193	0.218	-2.598
	BWO	Bi	4a	4.791	-0.272	0.620	-0.362	4.736	0.123	1.028	0.385
GGA-PBE+ $U_d+U_p$ +vdW	Bi	4a	4.791	0.272	0.620	0.362	4.735	-0.123	1.028	-0.385	4.251
	W	4a	8.357	0.002	0.502	-0.002	7.950	0.000	0.573	0.000	8.582
	O1	4a	-2.450	0.160	1.230	0.370	-2.190	0.222	1.262	0.506	-4.382
	O2	4a	-3.560	-2.058	-0.134	-2.187	-3.527	-0.099	-0.075	0.005	-1.657
	O3	4a	-3.560	2.058	-0.134	2.187	-3.528	0.173	-0.075	-0.004	-1.657
	O4	4a	-2.450	0.160	1.230	0.370	-2.190	0.223	1.262	0.506	-4.383
	O5	4a	-2.960	-0.320	0.405	0.256	-2.993	0.249	0.130	0.276	-2.502
O6	4a	-2.959	0.320	-0.405	-0.256	-2.993	0.249	-0.130	0.276	-2.502	